# Influence of Quantum Size Effects on Island Coarsening

C. A. Jeffrey,[1] E. H. Conrad,[2] R. Feng,[2] M. Hupalo,[3] C. Kim,[4] P. J. Ryan,[5] P. F. Miceli,[1] and M. C. Tringides[3]

[1]*Department of Physics and Astronomy, University of Missouri–Columbia, Columbia, Missouri 65211, USA*
[2]*The Georgia Institute of Technology, Atlanta, Georgia 30332-0430, USA*
[3]*Ames Laboratory, Iowa State University, Ames, Iowa 50011, USA*
[4]*Department of Physics and Research Institute of Basic Sciences, Kyunghee University, 1 Hoegi-dong Dongdaemoon-gu, Seoul 130-701, Korea*
[5]*MUCAT, Advanced Photon Source, Argonne National Laboratory, Argonne, Illinois 60439, USA*

(Received 28 September 2005; published 17 March 2006)

Surface x-ray scattering and scanning-tunneling microscopy experiments reveal novel coarsening behavior of Pb nanocrystals grown on Si(111)-(7 × 7). It is found that quantum size effects lead to the breakdown of the classical Gibbs-Thomson analysis. This is manifested by the lack of scaling of the island densities. In addition, island decay times $\tau$ are orders of magnitude faster than expected from the classical analysis and have an unusual dependence on the growth flux $F$ (i.e., $\tau \sim 1/F$). As a result, a highly monodispersed 7-layer island height distribution is found after coarsening if the islands are grown at high rather than low flux rates. These results have important implications, especially at low temperatures, for the controlled growth and self-organization of nanostructures.

DOI: 10.1103/PhysRevLett.96.106105 PACS numbers: 68.55.Ac, 81.16.Dn, 61.14.Hg, 68.35.Fx

Electron confinement in nanostructures gives rise to new quantized energy levels that are strongly dependent on the nanostructure's dimensions. This means that an object's size or shape is coupled to its total energy. This coupling is referred to as the quantum size effect (QSE) [1]. An example is the growth of Pb nanocrystalline islands on Si(111) [2–6]. In this system, the height distribution of the grown islands is found to peak in increments of two Pb layers. This bilayer stability is understood in terms of oscillations in the electronic energy as the discrete quantum states fall below the Fermi level approximately every two Pb layers [7–9]. While this energetic reason is the driving force for the observed height preference, it is unclear how the preferred islands are assembled and what role kinetic barriers play. The formation of the preferred islands is not exclusively controlled by thermodynamics, since these QSE islands are not in equilibrium.

The nucleation, growth, and coarsening of islands have been extensively described by a classical analysis [10]. In this scenario, the initial island nucleation is established by a steady state concentration of adatoms on the surface, which yields stable islands if they exceed a critical size of $i$ atoms. The island density $n$ is predicted and found to scale as the ratio $(F/D)^{\chi}$, where $\chi = i/(i+2)$, $D$ is the surface diffusion constant, and $F$ is the deposition rate [11]. Once the deposition flux is turned off, the island density slowly begins to decrease due to coarsening (Ostwald ripening), whereby a critical island radius $r_C$ is established such that islands having radii larger than $r_C$ will slowly grow at the expense of islands having smaller radii. This process, and its inherent dependence on island radius $r$, is controlled by the chemical potential difference between islands $\mu(r)$ and a 2D gas of adatoms $\mu_{\text{Free}}$, which is given by the Gibbs-Thomson relation: $\mu(r) - \mu_{\text{Free}} = 2\gamma/\omega r$ (where $\gamma$ is the surface tension of an island and $\omega$ is the atomic density of Pb) [12]. In particular, the Gibbs-Thomson relation was shown to accurately describe the situation for 2D islands on metal surfaces [10,13]. Such systems have been extensively studied in 2 and 3 dimensions and are well known to lead to scaling behavior for $r_C(t)$ that evolves at long times as a power law independent of the initial island density $n_0$ [10]. These scaling models give a time dependent island density;

$$n(t) = n_0(1 + t/\tau)^{-\beta}, \tag{1}$$

where $\tau \propto n_0^{-1/\beta}$ is a time constant and $\beta = 2/(m+2)$, with $m = 0, 1, 2$, depending on the dimensionality and kinetic processes at the island periphery. Note that, when $t \gg \tau$, $n(t) \propto t^{-\beta}$ independent of $n_0$.

As will be seen from the current experiments, most of the results for Pb/Si(111)-(7 × 7) do not conform to these classical predictions. Instead, they indicate that the role of QSE in island stability has a direct effect on coarsening in this system. Furthermore, these observations show the existence of novel and efficient pathways to self-organization that not only operate at much lower temperature but also result in sharper size distributions than those achievable through classical Ostwald ripening. Clearly, these pathways have important implications in the quest to identify robust and reproducible methods for atomic-scale control of nanostructures.

The x-ray experiments were performed in the surface x-ray scattering chamber at the 6ID-C $\mu$CAT beam line at Argonne National Laboratory using a 12.4 keV x-ray energy. The films were prepared *in situ* in ultrahigh vacuum ($p < 2 \times 10^{-10}$ torr). The Si(111)-(7 × 7) surface was prepared using standard techniques [14]. Coverages $\theta$ were determined as in Ref. [14] and are reported in units

 

of a bulk Pb(111) layer (i.e., 1.0 ML $= 9.43 \times 10^{14}$ atoms/cm$^2$). Island densities were determined by measuring the splitting of the diffuse scattering lobes (Henzler rings) [15] around the Pb(111) Bragg point [14]. This splitting $\Delta q_t$ is proportional to the mean island separation $L$, which is in turn proportional to the island density $n \sim 1/L^2 \sim (\Delta q_t/2\pi)^2$ [15,16]. This method of determining average island density is known to be accurate to first order [16]. The effect of lobe shape on the value of $n$ was found to be negligible as determined from 2D reciprocal space maps of the diffraction spots. The STM experiments were carried out in a variable temperature Omicron STM with Pb source calibration based on determining the optimal coverage for the dense Pb $-$ $\alpha$ $-$ $\sqrt{3} \times \sqrt{3}$ phase (i.e., 4/3 ML).

A number of striking features are revealed in Fig. 1, which presents the time evolution of the island density obtained from diffuse x-ray scattering after 1.2 ML of Pb was deposited on the Si(111)-(7 × 7) surface at 208 K for different flux rates. As can be seen, the island densities measured at different flux rates do not approach each other at long times. This is in sharp contradiction to the established scaling behavior of coarsening in Eq. (1) predicting converging island densities at long times (i.e., scaling independent of initial conditions). In fact, the initial island density shows little change with flux as shown in the lower inset in Fig. 1, suggesting that the differences in the curves are not driven by differences in the initial island density. This point is further amplified by comparing the coarsening times derived from fits to Eq. (1) using $\beta = 1$ (values of $1 \geq \beta \geq 0.7$ also gave acceptable fits). As shown in the upper inset in Fig. 1, the coarsening time is found to vary strongly with flux $\tau \propto F^{-1}$, which cannot be reconciled in terms of the initial island density. Both the lack of scaling and the $1/F$ dependence of $\tau$ are very robust, persisting to coverages up to 3 ML and over the entire temperature range where Pb islands form. We note that, while coarsening might be occurring during growth, standard coarsening models do not depend upon how an initial island density is established. In these experiments, it is clearly important *how* the initial density is produced, and this marks the breakdown of the standard models in this system. Thus, one is left to conclude that the deposition flux is directly responsible for the breakdown of the scaling expected from the Gibbs-Thomson effect.

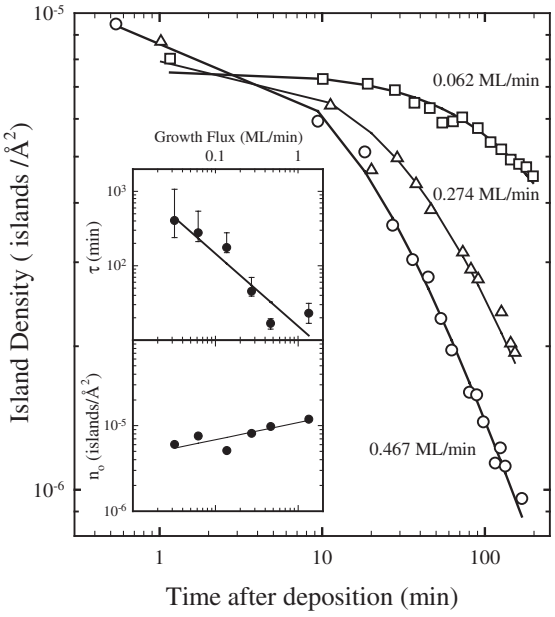


FIG. 1. Island density vs time demonstrates the breakdown of scaling: The curves do not approach each other at long times. These data were obtained from x-ray diffuse scattering measured after the deposition of 1.2 ML of Pb at 208 K for various deposition fluxes $F$. The solid curves are a fit to Eq. (1) with $\beta = 1$. The inset shows that the initial island density $n_0$ depends only weakly on flux $n_0 \propto F^{0.2}$, whereas the time constant changes quickly with flux $\tau \propto F^{-1}$.

The novelty of this coarsening is also manifested in the magnitude of the coarsening times that can be compared to those determined from Gibbs-Thomson driven decay previously measured on larger Pb crystals [17,18]. In those studies, the rate of decay of an island having radius $r$ positioned on a larger circular terrace of radius $\rho$ was well described by [19,20]:

$$\frac{dr}{dt} = \frac{-D_s \lambda_\beta}{r \ln(\rho/r)} \left( \frac{1}{r} - \frac{1}{\rho} \right), \tag{2}$$

where $D_s \lambda_\beta$ defines the detachment barrier of an atom from the island perimeter [$D_s \lambda_\beta = (7 \times 10^{13}/kT) \times e^{-0.86\ \mathrm{eV}/kT}$ eV nm$^3$/sec] [19]. In the limit $\rho \gg r$, the decay rate of an island then becomes $1/\tau \sim 3\pi^{3/2} D_s \lambda_\beta (n_0 h/\theta)^{3/2}$, where $\theta/n_0 h$ is the mean island area of $n_0$ islands/area at coverage $\theta$ with number of layers $h$. At 208 K, this gives $\tau \sim 10^6$ sec; $10^2$–$10^3$ times slower than observed in these experiments (see inset Fig. 1).

Insight into the reason for the breakdown of the Gibbs-Thomson effect and the fast decay time is obtained by looking at the specific heights of the islands from STM experiments performed under similar growth conditions as those in Fig. 1. Figure 2 shows a series of images as a function of time after depositing ~1.6 ML of Pb at 206 K at a high flux rate (0.5 ML/min). After 74 min, the overall island density decreases by a factor of 2.5, consistent with the x-ray data in Fig. 1. Note, however, that the initial island density is comprised of islands having a range of heights. Following the group of islands arranged in a crescent shape at the top left of the images, it is clear that the island heights evolve towards the superstable 7-layer islands. The 3-layer islands disappear extremely fast; the remaining 3-layer islands in Fig. 2(b) disappear in less than 2 min. These islands have approximately 1000 atoms in ~7.0 ± 0.4 nm diameter and, according to Eq. (2), should decay ~$10^4$ times slower than observed.

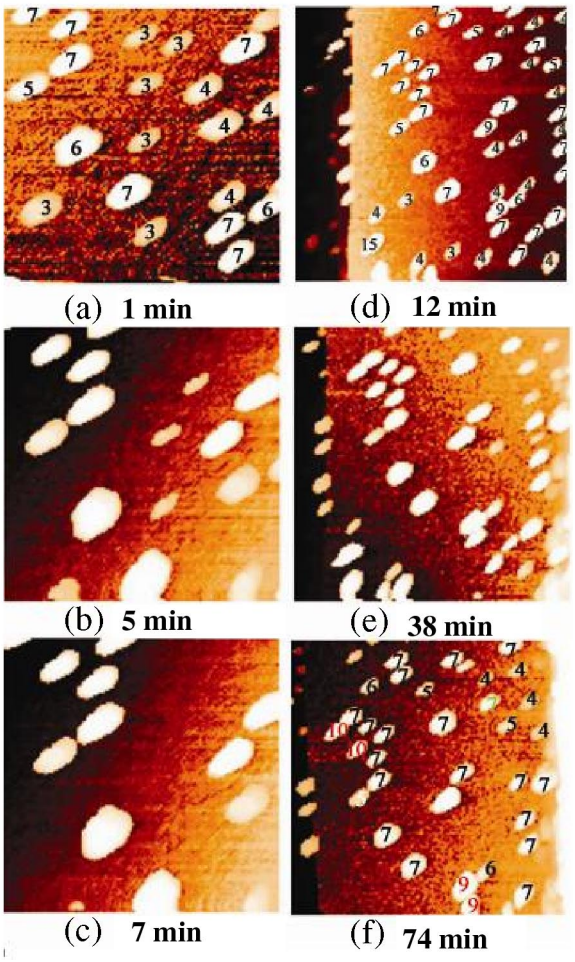


FIG. 2 (color online). STM images of the coarsening of 1.6 ML Pb deposited on Si(111)-$(7 \times 7)$ at 203 K at a flux of 0.5 ML/min. The times after deposition are shown for each image. The scale is $250 \times 250$ nm$^2$ for (a)–(c) and $500 \times 500$ nm$^2$ for (d)–(f). The tunneling parameters were 2 V at 1 nA. Scans take 0.5 min each. The island height is marked on top of each island for (a), (d), and (f) (height is measured with respect to the Pb wetting layer [14].) It can be seen that 3-layer islands are less stable than 4-layer ones and both of these are less stable than 7-layer islands.

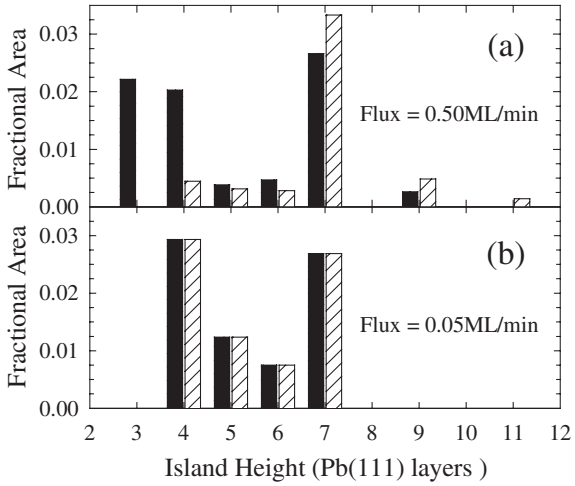


FIG. 3. Histograms of the island height distribution for 1.6 ML grown at 203 K, measured 5 min after (black) and 74 min after deposition (cross-hatched). (a) shows a high flux rate deposition, 0.5 ML/sec, leading to a broad initial island height distribution with fast decay of unstable islands. (b) shows a low flux deposition, 0.05 ML/min, leading to a narrower initial island height distribution with little change over time.

Clearly, atoms detach from these islands and diffuse until they are incorporated into the surrounding 7-layer islands. The majority of the 4-layer islands also disappear (some transform into higher height islands) but over a longer time scale compared to the 3-layer island decay time.

To be more quantitative, we have measured height histograms of Pb islands before and after coarsening for both low and high flux rates at 206 K. Figure 3(a) shows the height histogram for a 1.6 ML film grown at $F = 0.5$ ML/min both 5 min after deposition and 74 min later. The initial surface exhibits a relatively broad distribution of island heights, which remarkably evolve to a single dominant population at 7 layers [6]. Populations having heights less than 7 layers decrease significantly after coarsening, especially the 3- and 4-layer islands. In contrast, the same amount deposited at a lower flux rate (0.05 ML/min), shown in Fig. 3(b), exhibits a relatively narrower initial height distribution. Within measurement statistics, this distribution remains unchanged even after 80 min. We note that the island density for the film in Fig. 3(b) remains essentially constant during the 80 min coarsening experiment. This and the data in Fig. 2 are consistent with the observed x-ray result that low flux islands coarsen slower. Figures 1 and 3 demonstrate that growth at high flux rates ultimately leads to a sharper monodispersed height distribution as well as a lower density, in stark contrast to the usual situation in epitaxial growth.

The experiments described above suggest the following picture for the growth of QSE nanocrystals. The initial island nucleation exhibits a weak dependence on the deposition flux, as in standard nucleation theory, although the exponent we observe, $\chi = 0.2$, is slightly smaller than predicted by those theories. The types of islands that are produced, however, depend strongly on the flux rate. High flux rates generate a broader range of island heights (having a broader range of stability), presumably because of the larger adatom concentration that drives a higher chemical potential. Thus, many of the islands are unstable and decay once the deposition flux is turned off. This quickly leads to a significantly lower island density. Conversely, lower flux rates generate a narrower height distribution of the more stable islands that decay slowly in time. For example, 3-layer islands are less stable than 4-layer islands and both of these are less stable than 7-layer islands. Correspondingly, the 3-layer islands decay very quickly at high

flux followed by the 4-layer islands. At low flux, the 3-layer islands do not appear at all. It is curious that the 4-layer islands generated at low flux are not observed to decay. This could be related to the fact that these islands are larger in diameter. The average size of the 4-layer islands is 40 nm for low flux versus 18 nm for high flux rates. Thus, there could be a height-dependent critical lateral size defining whether a 4-layer island will decay or not. To account for the extremely fast decay times observed at high flux rates, collective effects must be operating (where the detachment of a single atom can trigger highly correlated detachment of many more atoms). Although the microscopic origin of such processes still needs to be identified, they have tremendous implications about the self-organization in the epitaxial growth of nanocrystals.

In summary, the nucleation and coarsening of Pb islands grown on Si(111)-(7 $\times$ 7) were studied to clarify the role of QSE in the final island morphology after coarsening. Surprisingly, improved height and size distributions along with a much lower island density are observed after deposition at high rather than low flux rates, contrary to the classical scaling theory of nucleation and Ostwald ripening. The breakdown of the Gibbs-Thomson effect that determines stability in terms of the island diameter is manifested in the lack of scaling of the island density as well as the remarkably fast time scales of the island decay. The evaporation of unstable 3-layer islands with 1000 atoms within less than 2 min suggests the presence of another far more efficient decay mechanism operating at low temperatures that is related to QSE. These discoveries have important ramifications for the controlled growth of nanostructures, especially at low temperatures, because they challenge standard wisdom and expectations in the field.

The Advanced Photon Source is supported by the DOE Office of Basic Energy Sciences, Contract No. W-31-109-Eng-38. The $\mu$-CAT beam line is supported through Ames Laboratory, operated for the U.S. DOE by Iowa State University under Contract No. W-7405-Eng-82. Research funding was supported, in part, by Ames Laboratory (M. C. T.), Canim Scientific Group (E. H. C.), the Missouri University Research Board, the National Science Foundation DMR-0405742, and the Petroleum Research Fund No. 41792AC10 (P. F. M., C. A. J., C. K.), the Natural Sciences and Engineering Research Council (NSERC) of Canada (C. A. J.), the Center for Nanostructured Materials Technology under 21st Century Frontier R&D Programs of the Ministry of Science and Technology (No. 05K1501-02520), Korea (C. K.).

[1] M. Jalochowski, M. Hoffmann, and E. Bauer, Phys. Rev. B **51**, 7231 (1995).
[2] K. Budde, E. Abram, V. Yeh, and M. C. Tringides, Phys. Rev. B **61**, R10 602 (2000).
[3] H. Yu, C. S. Jiang, Ph. Ebert, X. D. Wang, J. M. White, Q. Niu, Z. Zhang, and C. K. Shih, Phys. Rev. Lett. **88**, 016102 (2002).
[4] W. B. Su, S. H. Chang, W. B. Jian, C. S. Chang, L. J. Chen, and Tien T. Tsong, Phys. Rev. Lett. **86**, 5116 (2001).
[5] A. Mans, J. H. Dil, A. R. H. F. Ettema, and H. H. Weitering, Phys. Rev. B **66**, 195410 (2002).
[6] M. Hupalo, S. Kremmer, V. Yeh, L. Berbil-Bautista, E. Abram, and M. C. Tringides, Surf. Sci. **493**, 526 (2001).
[7] H. Hong, C.-M. Wei, M. Y. Chou, Z. Wu, L. Basile, H. Chen, M. Holt, and T.-C. Chiang, Phys. Rev. Lett. **90**, 076104 (2003).
[8] Z. Zhang, Q. Niu, and C-K. Shih, Phys. Rev. Lett. **80**, 5381 (1998).
[9] C. M. Wei, and M. Y. Chou, Phys. Rev. B **66**, 233408 (2002).
[10] M. Zinke-Allmang, L. C. Feldman, and M. H. Grabow, Surf. Sci. Rep. **16**, 377 (1992).
[11] A. Venables, G. D. T. Spiller, and M. Hanbucken, Rep. Prog. Phys. **47**, 399 (1984).
[12] P. Wynblatt and N. A. Gjostein, Prog. Solid State Chem. **9**, 21 (1975).
[13] K. Morgenstern, G. Rosenfeld, E. Lægsgaard, F. Besenbacher, and G. Comsa, Phys. Rev. Lett. **80**, 556 (1998).
[14] R. Feng, E. H. Conrad, M. C. Tringides, C. Kim, and P. F. Miceli, Appl. Phys. Lett. **85**, 3866 (2004).
[15] P. O. Hahn, J. Clabes, and M. Henzler, J. Appl. Phys. **51**, 2079 (1980).
[16] H. Durr, J. F. Wendelken, and J.-K. Zuo, Surf. Sci. **328**, L527 (1995).
[17] M. Nowicki, C. Bombis, A. Emundts, and H. P. Bonzel, Phys. Rev. B **67**, 075405 (2003).
[18] J. G. McLean, B. Krishnamachari, D. R. Peale, E. Chason, J. P. Sethna, and B. H. Cooper, Phys. Rev. B **55**, 1811 (1997).
[19] K. Thurmer, J. J. Reuut-Robey, E. D. Williams, M. Uwaha, A. Emundts, and H. P. Bonzel, Phys. Rev. Lett. **87**, 186102 (2001).
[20] M. Uwaha, J. Phys. Soc. Jpn. **57**, 1681 (1988).